ANZIAM J. **65** (2023), 135–154
doi:10.1017/S1446181123000081

FLIGHT LIMITATIONS IMPOSED ON SINGLE ROTOR AND COAXIAL HELICOPTERS BY THE LIFT EQUATION

B. MALDON[1] and MICHAEL H. MEYLAN[1]✉

(Received 28 February, 2023; accepted 23 May, 2023; first published online 17 July, 2023)

Abstract

To compute the maximum speed threshold for helicopters, we model the lift produced by the rotor blades. Using this model, we derive limits for each method traditionally used to alleviate dissymmetry of lift. Additionally, we find the minimum rotor angular velocity required to produce a prescribed lift at a given forward velocity. We derive conditions on the coefficient of lift for helicopter airfoils that maintain altitude. Further considerations are also made with regard to the properties of the air and its effect on helicopter dynamics.

2020 *Mathematics subject classification*: 76G25.

Keywords and phrases: equation of lift, helicopter dynamics, dissymmetry of lift.

1. Introduction

Helicopters remain a vital component of aviation technology, first realised in Igor Sikorsky's VS300 model, which was the first successful helicopter to feature a main rotor and tail rotor [1]. La Mantia and Dabnichki calculated optimal airfoil thicknesses based on the standard NACA airfoil shapes [4]. Kulchenko et al. applied mathematical models for single-rotor helicopters for autopilot technology in 2014 [3]. Finally, Romani and Casalino elucidated the influence of rotor-induced vortices on the overall production of lift on the helicopter blades [10]. The theory of helicopter dynamics encompasses the study of the complex aerodynamic and mechanical principles that govern the flight of helicopters. Helicopters are unique aircraft that rely on the interaction between components, including the main rotor, tail rotor, fuselage and various control systems, to achieve controlled vertical takeoff, landing and manoeuvrability

[1]School of Information and Physical Sciences, University of Newcastle, Callaghan, NSW 2308, Australia; e-mail: benjamin_maldon@outlook.com, mike.meylan@newcastle.edu.au

in the air. The aerodynamics of helicopter rotors involve lift, drag, induced flow and rotor wake, which are influenced by blade geometry, airfoil design and rotor speed. Understanding the dynamic behaviour of helicopters requires knowledge of key concepts such as cyclic and collective pitch control, autorotation, ground effect and gyroscopic precession. Numerous scientific studies and engineering advancements have contributed to the development and refinement of helicopter dynamics, many of which can be found in [2, 5].

Perdomo and Wei studied blade flapping in their paper [9], providing a time-dependent truncated Fourier series to calculate the flapping angle for an airfoil across the rotor disk. Majhi and Ganguli studied dynamic stall and the efficacy of assuming small flapping angles in mathematically modelling helicopters [7].

Applications for airfoils extend beyond aviation technology for helicopters. Liu et al. recently used a dynamic stall model to study wind turbines for renewable energy applications [6]. Rozhdestvinsky and Ryzhov completed a survey for flapping-wing propulsors as they apply to aerohydrodynamics in 2003 [11].

We define a helicopter's fundamental components to capture the limiting factors arising from flying helicopters at high forward velocities. Primarily, this paper will study the lift equation as a model for the thrust collectively produced by the helicopter blades.

1.1. Helicopter rotor blades During operation, helicopter rotor blades spin about the rotor shaft at a typically constant speed Ω_R (usually measured in RPM). We will assume all rotor blades rotate anticlockwise, with the exception of the second rotor disk of a coaxial helicopter or when otherwise noted. Each blade, therefore, has an angular velocity Ω of

$$\Omega = \frac{\pi\Omega_R}{30}.$$

Given a helicopter rotor disk of n blades, the azimuth angle θ for blade k of n at time t is given by

$$\theta(t) = \Omega t + \frac{2\pi(k-1)}{n},$$

so that at time $t = 0$, the first helicopter blade in the rotor disk is in the advancing position. Using the azimuth angle, the tip B_{tip} of blade k of n at time t is therefore given by

$$B_{\text{tip}} = R[\cos(\theta), \sin(\theta), 0],$$

where R is the length of the helicopter blade (and, therefore, the radius of the rotor disk).

1.2. Dissymmetry of lift Under static hover conditions, the lift is generated uniformly across the rotor disk as the blades pass through the air. When helicopter blades are subject to a relative wind (usually induced by the forward velocity of the helicopter), more lift is generated on the advancing side of the rotor disk and less lift

https://doi.org/10.1017/S1446181123000081 Published online by Cambridge University Press

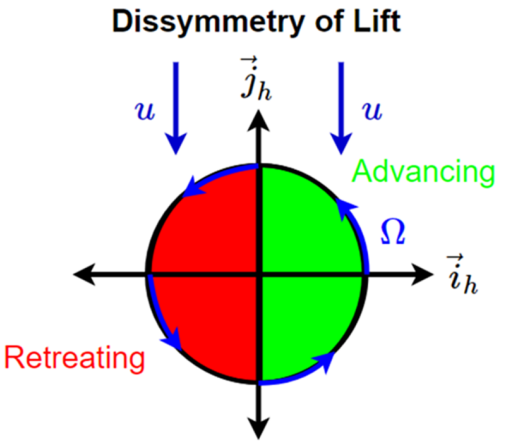

FIGURE 1. Diagram showing the direction of rotation with the relative wind.

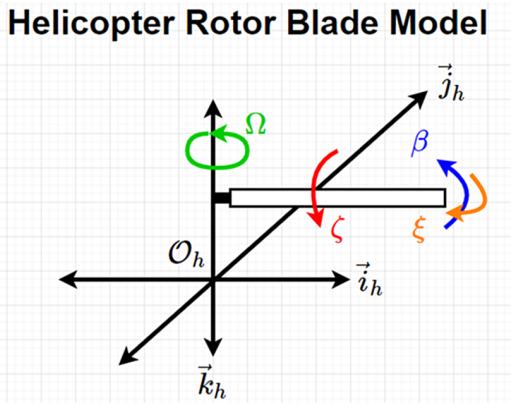

FIGURE 2. Diagram of the three angles of rotation for a helicopter rotor blade.

is generated on the retreating side. This dissymmetry of lift is detailed in Figure 1 and shows a fundamental problem encountered by single-rotor helicopters. Coaxial helicopters amend this issue with their unique counter-rotating disks.

1.3. Helicopter rotor blade airfoils To combat the dissymmetry of lift, helicopter rotor blades may rotate about three axes, as shown by Figure 2. The lead-lagging angle ξ, flapping angle β and feathering angle ζ are all used to decrease the lift on the advancing blades and increase lift on the retreating blades.

The primary limitations of these measures are found in retreating blade stall and supersonic blade limitations. Figure 3 shows the effect of the retreating blade stall

https://doi.org/10.1017/S1446181123000081 Published online by Cambridge University Press

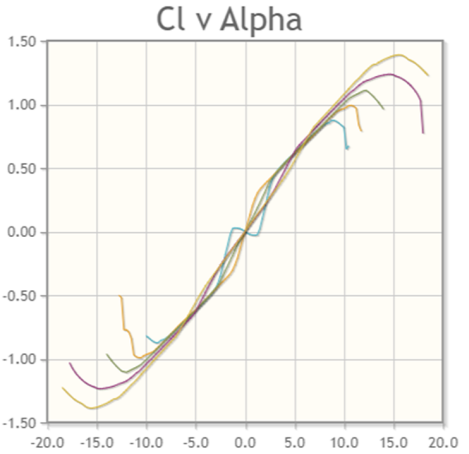

FIGURE 3. Plot of the coefficient of lift against the angle of attack for the NACA0012 airfoil for Reynolds numbers from 5×10^5 to 10^6 [8]. The x-axis is in degrees.

coefficient of lift for a NACA0012 airfoil. Once the angle of attack α approaches its critical value α_c, the lift increase plateaus and leads to decreased lift if the angle of attack exceeds the critical value.

In the problem of supersonic blade limitations, helicopter rotor blade tips cannot exceed the speed of sound without encountering excessive drag and air resistance liable to break the blades. Mathematically, the angular velocity Ω of the blades must satisfy

$$\Omega R + u < v,$$

where v is the speed of sound. Rearranging for Ω, we have

$$\Omega = \eta \frac{v - u}{R}, \tag{1.1}$$

where $\eta < 1$ is a tolerance factor. Unless otherwise stated, we will assume $\eta = 1$ for theoretical calculations to obtain the maximum possible lift.

2. Mathematical model

In this section, we model the lift produced by helicopter blade k of n with the standard lift equation

$$\ell_{\text{std}} = \tfrac{1}{2}\rho c v^2 C_L, \tag{2.1}$$

where ℓ_{std} is the lift per unit length, ρ is the air density, c is the chord length, v is the velocity of the blade and C_L is the coefficient of lift. In this study, we will consider the lift generated by one blade with azimuth angle $\theta = \Omega t$. We are assuming uniform chord along blade, straight blades and uniform angle of attack.

https://doi.org/10.1017/S1446181123000081 Published online by Cambridge University Press

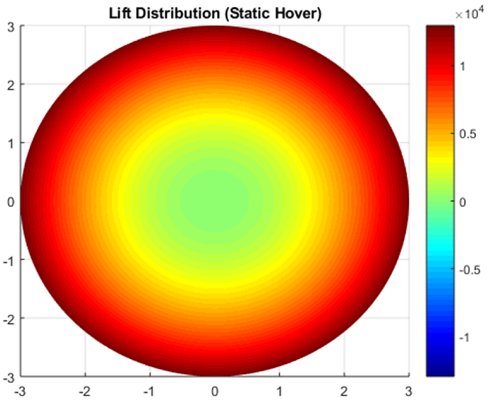

FIGURE 4. Lift distribution of the rotor disk in standard hover.

2.1. Assumptions and parameter values We will only consider the lift generated on the disk with polar coordinates. For time-dependent effects during operation, we will use the azimuth angle expression

$$\theta(t) = \Omega t + \frac{2\pi(k-1)}{n}.$$

The coefficient of lift C_L is regarded to be a function of angle of attack α only. We will assume C_L is either constant or linear with respect to α, based on Figure 3.

Throughout this paper, the rotor blades have a length 3 m and a chord length of 180 mm (or 0.18 m). The default mass of the helicopter is 1000 kg.

For reference, we will use the NACA0012 airfoil [8] for the coefficient of lift computations. Other airfoils will also be compatible with these expressions, given the lift coefficients as functions of the angle of attack and Reynolds number.

2.2. Standard lift equation Recall the standard lift equation is given by

$$\ell_{\text{std}} = \tfrac{1}{2}\rho c v^2 C_L.$$

To study the effect of a relative wind, we model the linear velocity with the equation

$$v = \Omega r + u\cos(\theta),$$

where u is the relative wind speed and θ is the blade azimuth angle. The lift becomes a function of the position on the blade $r \in [0, R]$ and azimuth angle $\theta \in [0, 2\pi)$.

Figure 4 shows the lift distribution for a helicopter rotor blade in static hover using equation (2.1). In the absence of relative wind, the lift is equal across the rotor disk. The lift is maximized at the tip of the rotor disk due to the maximal linear velocity at the blade tips.

Figure 5 shows the lift distribution for a helicopter rotor blade under the relative winds $u = 50\,\text{ms}^{-1}$ and $u = 120\,\text{ms}^{-1}$, using equation (2.1). Without adjusting the angle

https://doi.org/10.1017/S1446181123000081 Published online by Cambridge University Press

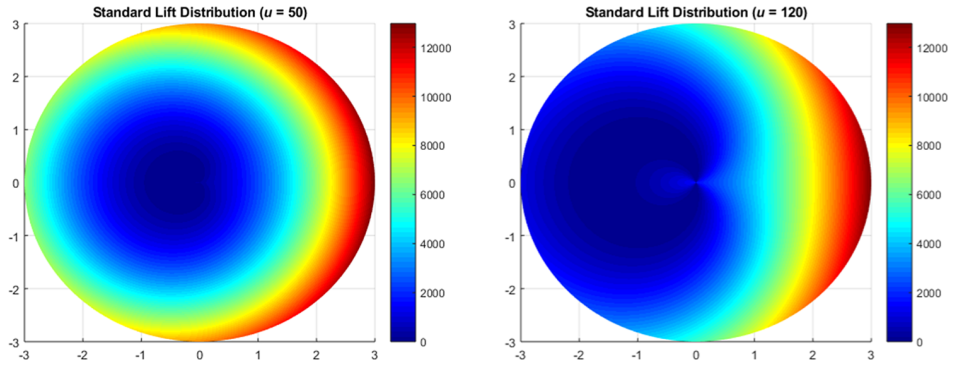

FIGURE 5. Lift distribution of the rotor disk given a relative wind $u = 50\,\mathrm{ms}^{-1}$ (left) and $u = 120\,\mathrm{ms}^{-1}$ (right).

of attack, the relative wind decreases the lift produced on the retreating side of the rotor disk.

3. Results

3.1. Revised lift equation In this section, we compute the lift generated by a helicopter rotor blade with the modified equation

$$L_{\mathrm{mod}}(u,\theta) = \int_0^R \frac{\rho c C_L}{2}(\Omega r + u\cos(\theta))|\Omega r + u\cos(\theta)|\,dr.$$

Similar expressions can be found in [2, 5]. Expressing the velocity term as $v|v|$ rather than v^2 allows the term to become negative, as experienced by retreating blades at high velocity. Upon explicit calculation,

$$L_{\mathrm{mod}}(u,\theta) = \frac{\rho c C_L}{6\Omega}[(\Omega R + u\cos(\theta))^2|\Omega R + u\cos(\theta)| - u^3\cos^2(\theta)|\cos(\theta)|].$$

3.1.1. Retreating blade special case For retreating blades ($\theta = 180°$), the lift generated simplifies to

$$L_{\mathrm{mod},R}(u) = \frac{\rho c C_L}{6\Omega}[(\Omega R - u)^2|\Omega R - u| - u^3].$$

Given $\Omega = (v - u)/R$ to ensure maximum RPM, the lift becomes

$$L_{\mathrm{mod},R}(u) = \frac{R\rho c C_L}{6(v-u)}[(v-2u)^2|v-2u| - u^3].$$

To find u such that $L_R(u) = 0$, we solve

$$[(v-2u)^2|v-2u| - u^3] = 0.$$

https://doi.org/10.1017/S1446181123000081 Published online by Cambridge University Press

Given $u < v/2$,

$$u = \frac{v}{3}.$$

Given $v = 343\ \mathrm{ms}^{-1}$, we see that traditional helicopters cannot exceed $v/3 \approx 114.3\ \mathrm{ms}^{-1}$. This limit is slightly higher than the known world speed record of $111.35\ \mathrm{ms}^{-1}$ by the Westland Lynx set in 1986 [1].

3.1.2. Negative lift region If $u > v/3$, a region of the rotor disk about the tip of the retreating blade will produce negative lift when integrated. To find this region, we solve $L(u, \theta_c) = 0$ for θ_c given $u > v/3$. That is, we solve

$$\frac{\rho c C_L}{6\Omega}[(\Omega R + u\cos(\theta_c))^2|\Omega R + u\cos(\theta_c)| - u^3\cos^2(\theta_c)|\cos(\theta_c)|] = 0.$$

Letting $\epsilon = \cos(\theta_c)$ and using $\Omega = (v - u)/R$,

$$(v - u(1-\epsilon))^2|v - u(1-\epsilon)| - u^3\epsilon^2|\epsilon| = 0.$$

Since $\epsilon < 0$, by expansion and factoring,

$$\left(\frac{v-u}{u}\right)(2\epsilon + v)\left(\epsilon - 2\frac{v-u}{u}\right) = 0.$$

Therefore, we have $\epsilon = (v - u)/2u$. Upon substitution,

$$\theta_c = \arccos\left(\frac{v-u}{2u}\right).$$

Therefore, the helicopter blades will produce negative lift for azimuth angles, satisfying

$$\theta \in \left[\pi - \arccos\left(\frac{v-u}{2u}\right), \pi + \arccos\left(\frac{v-u}{2u}\right)\right].$$

3.2. Modified lift equation To recapture the loss of lift on the retreating rotor blades, we modify the lift equation to be

$$\ell_{\mathrm{mod}} = \tfrac{1}{2}\rho c v|v| C_L, \tag{3.1}$$

replacing v^2 with $v|v|$. This allows the velocity of the blade to take negative values, which will occur on the retreating side for sufficiently high relative wind speeds. The lift distribution in static hover matches Figure 4 as $v = \Omega r$. Given a relative wind u, we set $v = \Omega r + u\cos(\theta)$ as before. Figure 6 shows that the relative wind greatly affects the lift produced near the rotor shaft on the retreating side.

3.2.1. Modified integrated lift equation Using the same techniques as the standard lift equation, we may calculate the total lift produced by a helicopter rotor blade by integrating the lift over the blade. That is, we compute

$$L(\alpha, u, \theta) = \int_0^R \frac{1}{2}\rho c(\Omega r + u\cos(\theta))|\Omega r + u\cos(\theta)| C_L(\alpha)\, dr.$$

https://doi.org/10.1017/S1446181123000081 Published online by Cambridge University Press

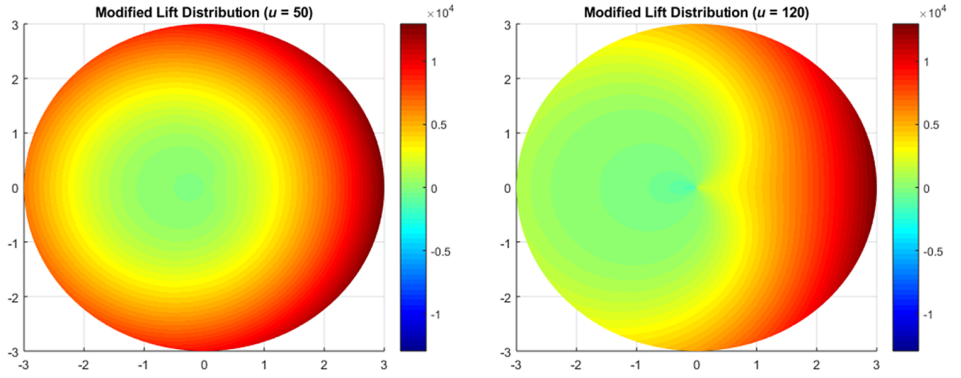

FIGURE 6. Modified lift distribution of the rotor disk given a relative wind $u = 50\,\mathrm{ms}^{-1}$ (left) and $u = 120\,\mathrm{ms}^{-1}$ (right).

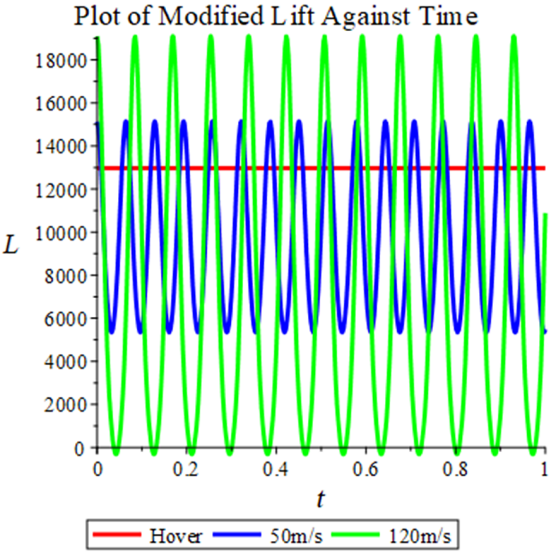

FIGURE 7. Plot of the lift generated over time for several forward velocities.

Upon computation,

$$L(\alpha, u, \theta) = \frac{\rho c C_L(\alpha)}{6\Omega}[(\Omega R + u\cos(\theta))^2|\Omega R + u\cos(\theta)| - u^3\cos^2(\theta)|\cos(\theta)|].$$

With $\Omega = (v - u)/R$, the lift becomes

$$L(\alpha, u, \theta) = \frac{R\rho c C_L(\alpha)}{6(v - u)}[(v - u + u\cos(\theta))^2|v - u + u\cos(\theta)| - u^3\cos^2(\theta)|\cos(\theta)|].$$

Figure 7 plots the lift generated by the blade over time using the usual azimuth angle $\theta(t) = \Omega t$. The lift oscillates as the blade transitions between advancing and retreating.

https://doi.org/10.1017/S1446181123000081 Published online by Cambridge University Press

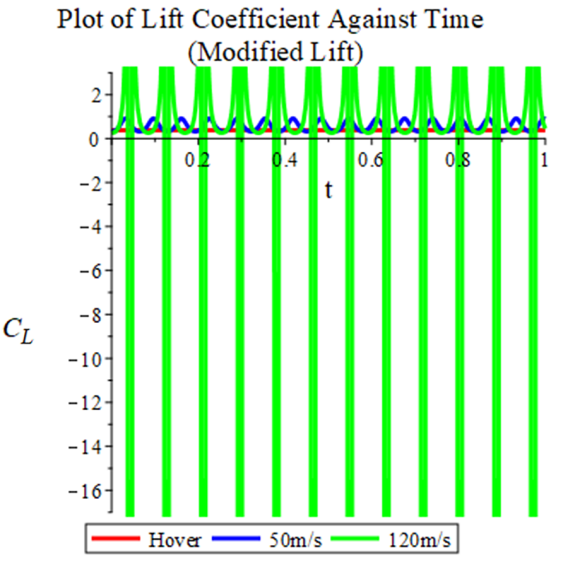

FIGURE 8. Plot of the lift coefficient C_L required for vertical hover against time.

As the forward velocity increases, the oscillation amplitude increases and the centre decreases. As the velocity may take negative values with the expression $v|v|$, we see the special case $u = 120\,\mathrm{ms}^{-1}$ produces negative lift at the retreating side.

To ensure $L = mg/n$ for vertical hover, the coefficient of lift must satisfy

$$C_L(\alpha) = \frac{6\Omega mg}{\rho cn}[(\Omega R + u\cos(\theta))^2|\Omega R + u\cos(\theta)| - u^3\cos^2(\theta)|\cos(\theta)|]^{-1}.$$

With $\Omega = (v - u)/R$, the coefficient of lift becomes

$$C_L(\alpha) = \frac{6\eta(v-u)mg}{\rho Rcn} \times [(\eta(v-u) + u\cos(\theta))^2|\eta(v-u) + u\cos(\theta)| - u^3\cos^2(\theta)|\cos(\theta)|]^{-1}.$$

Figure 8 is a plot of the coefficient of lift over time given the standard azimuth angle $\theta(t) = \Omega t$. For static hover and the relatively low forward velocity $50\,\mathrm{ms}^{-1}$, we see the coefficient of lift take reasonable values between 0 and 1. For the forward velocity $120\,\mathrm{ms}^{-1}$, we see that the negative lift produced on the retreating side leads to discontinuities the coefficient of lift cannot reconcile. The angle of attack is, therefore, unable to balance the lift on the retreating side for forward velocities $u > v/3$.

3.3. Average modified lift To better understand the lift performance of the helicopter blade over the entire rotor disk, we also compute the average lift produced over

https://doi.org/10.1017/S1446181123000081 Published online by Cambridge University Press

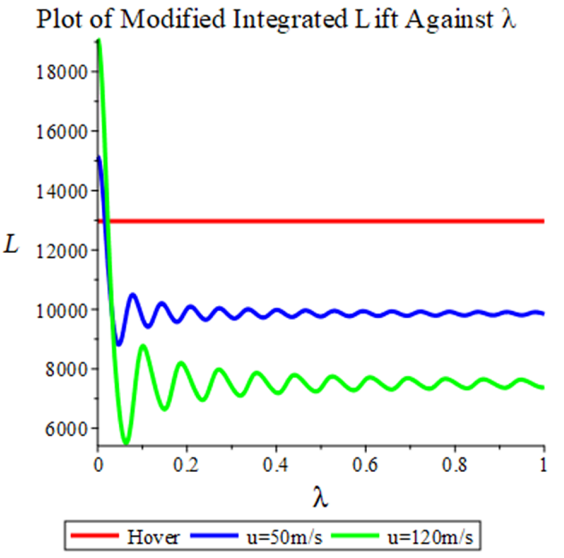

FIGURE 9. Plot of the average lift $L_{\text{mod},T}$ over time interval λ.

time λ with the expression

$$L_{\text{mod},\lambda} = \frac{1}{\lambda}\int_0^{\lambda}\int_0^{R}\frac{1}{2}\rho c(\Omega r + u\cos(\Omega t))|\Omega r + u\cos(\Omega t)|C_L(\alpha)\,dr\,dt.$$

We compute this integral numerically with a standard midpoint Riemann sum with 300 evenly spaced intervals in Figure 9. As the forward velocity increases, the negative lift produced by the retreating side lowers the average lift across the disk. A higher forward velocity results in a more significant difference.

3.4. Average lift across rotor disk Since the helicopter rotor speed Ω is dependent on u, the time interval required to consider one revolution is also dependent on u. Therefore, for the standard lift equation, we compute the average value over one particular revolution with the alternative integral

$$L_{\text{std},T}(u) = \frac{1}{2\pi}\int_0^{2\pi}\int_0^{R}\frac{1}{2}\rho c\left(\frac{\nu - u}{R}r + u\cos(\theta)\right)^2 C_L\,dr\,d\theta.$$

Upon simplification,

$$L_{\text{std},T}(u) = \frac{\rho c R C_L(\alpha)}{12}[5u^2 - 4\nu u + 2\nu^2].$$

For the modified lift, we compute

$$L_{\text{mod},T}(u) = \frac{1}{2\pi}\int_0^{2\pi}\int_0^{R}\frac{1}{2}\rho c\left(\frac{\nu - u}{R}r + u\cos(\theta)\right)\left|\frac{\nu - u}{R}r + u\cos(\theta)\right|C_L\,dr\,d\theta.$$

https://doi.org/10.1017/S1446181123000081 Published online by Cambridge University Press

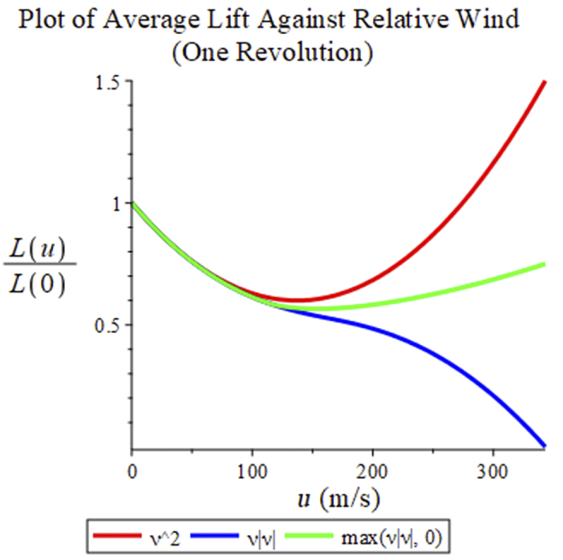

FIGURE 10. Plot of the normalized average lift over forward velocity for each model.

Finally, to reconcile the negative lift from the modified velocity model $v|v|$, we also compute the integral

$$L_{\max,T} = \frac{1}{2\pi}\int_0^{2\pi}\int_0^R \max\left(\frac{1}{2}\rho c\left(\frac{v-u}{R}r + u\cos(\theta)\right)\left|\frac{v-u}{R}r + u\cos(\theta)\right|C_L, 0\right) dr\, d\theta.$$

To better understand the lift differences, we scale the result by the lift obtained in static hover. From Figure 10, we find the models produce similar average lifts for low forward velocity as the effect of dissymmetry of lift is at its lowest influence.

As the forward velocity increases, the lift produced by the blade decreases as the rotor speed Ω must decrease. Once the negative lift is produced by the retreating blade at $u = v/3$, we find the lift from the standard and modified model diverge. The standard model increases lift as the forward velocity remains nonnegative. For the modified model, the overall lift decreases as the negative lift on the retreating blades counteracts the positive lift produced by the advancing sides. If the angle of attack can be set to 0°, the negative effect of the retreating blade diminishes and the lost lift begins to recover.

Since the retreating side of the rotor disk cannot produce any positive lift for velocities above 114.3 ms^{-1}, we find that only coaxial helicopters are able to rectify the issue. We also note the lift produced in these velocities varies between 50% and 75% of the lift generated in static hover. This is primarily a consequence of the decreased rotor speed Ω as u increases.

3.5. Minimum rotor speed requirements To obtain the maximum lift attainable from helicopter blades, we prescribe Ω with equation (1.1) to the lift equation (3.1). To find the minimum requirements for Ω to hold a given lift L, we estimate (to enable us

https://doi.org/10.1017/S1446181123000081 Published online by Cambridge University Press

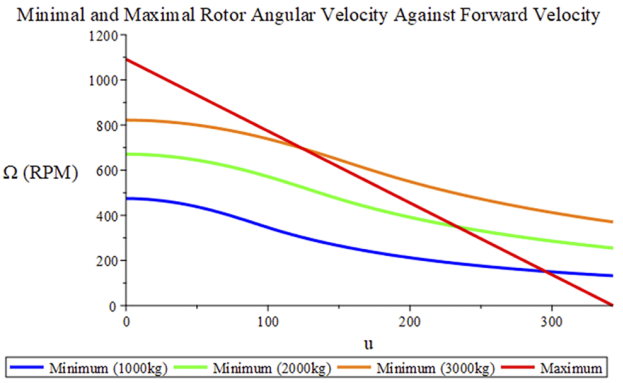

FIGURE 11. Plot of minimum Ω for various weights with the theoretical maximum against forward velocity.

to give an approximate analytic formula) the average lift by

$$L_{\text{avg}}(u,\Omega) = \frac{1}{4}\left[L(u,0,\Omega) + 2L\left(u,\frac{\pi}{2},\Omega\right) + L(u,\pi,\Omega)\right],$$

which simplifies to

$$L_{\text{avg}}(u,\Omega) = \frac{\rho c}{24\Omega}[(\Omega R+u)^3 + (\Omega R-u)^2|\Omega R-u| + 2\Omega^3R^3 - 2u^3].$$

Solving for Ω,

$$\Omega(u,L) = \begin{cases} 2^{-2/3}\dfrac{2^{7/3}L - 2^{1/3}(Rc\rho u^2) + ((Rc\rho u^2)^{3/2}+K)^{2/3}}{R\sqrt{Rc\rho}((Rc\rho u^2)^{3/2}+K)^{1/3}}, & u < \sqrt{\dfrac{3L}{c\rho R}}, \\ -\dfrac{3u}{2R} + \dfrac{\sqrt{3c\rho R(16L+3c\rho Ru^2)}}{2c\rho R^2}, & u \geq \sqrt{\dfrac{3L}{c\rho R}}, \end{cases} \tag{3.2}$$

where $K = \sqrt{-128L^3 + 96(Rc\rho u^2)L^2 - 24(Rc\rho u^2)^2L + 3(Rc\rho u^2)^3}$.

From Figure 11, we see that the minimum threshold for Ω decreases as forward velocity u increases. While this will allow the rotor disk to spin at a lower RPM, the maximum threshold imposed by equation (1.1) decreases at a faster rate. Consequently, the interval between the maximum and minimum values for Ω decreases in length until they coincide at some $u = u_M(L)$ dependent on the lift L required by the minimum threshold.

By solving $\Omega(u_M, L) = (v - u_M)/R$, we are able to find the maximum allowable speed limit as imposed by the minimum lift L that the rotor disk(s) must generate. Assuming $u_M > 3L/c\rho R$, we find the maximum speed limit is given by

$$u_M(L) = \frac{v}{4} + \frac{\sqrt{3Rc\rho(3Rc\rho v^2 - 32L)}}{4Rc\rho}. \tag{3.3}$$

https://doi.org/10.1017/S1446181123000081 Published online by Cambridge University Press

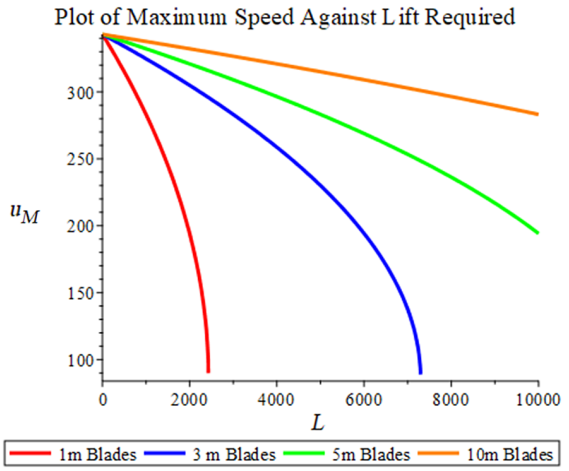

FIGURE 12. Plot of maximum speed u_M against lift L for several blade lengths.

In Figure 12, we plot the maximum speed limit as a function of lift required for a variety of helicopter blade lengths. If the forward velocity of a helicopter should exceed this limit (if $u > u_M$), the rotor angular velocity Ω must decrease, and the lift produced will not be sufficient to maintain altitude. To compensate for this, other methods for producing lift will be necessary, such as wings or a modified fuselage shape.

We note in equation (3.3) that u_M attains its minimum at $L = 3Rc\rho v^2/32$, where $u_M = v/4$.

3.6. Lift on the advancing side of the rotor disk To study the effect of the relative wind on the advancing side of the rotor disk, we calculate the integral

$$L_{\text{adv}}(u) = \int_{-\pi/2}^{\pi/2} \int_0^R \frac{1}{2\pi} \rho c(\Omega r + u\cos(\theta))|\Omega r + u\cos(\theta)|\, dr\, d\theta.$$

Since $\Omega r + u\cos(\theta) > 0$ for advancing rotor blades and the integral is even, we may simplify the expression to

$$L_{\text{adv}}(u) = \frac{2}{\pi} \int_0^{\pi/2} \int_0^R \frac{1}{2} \rho c(\Omega r + u\cos(\theta))^2\, dr\, d\theta.$$

Upon simplification,

$$L_{\text{adv}}(u) = \frac{R\rho c}{12\pi}[3\pi u^2 + 12\Omega R u + 2\pi(\Omega R)^2].$$

In Figure 13, we plot L_{adv} against u for the maximum theoretical Ω prescribed by equation (1.1) and for the minimum values for Ω required to maintain altitude for 1000 kg, 2000 kg and 3000 kg helicopters. As the forward velocity increases, it reaches the maximum allowable limit u_M, at which point the lift generated coincides with the lift obtained by the maximal rotor angular velocity Ω.

https://doi.org/10.1017/S1446181123000081 Published online by Cambridge University Press

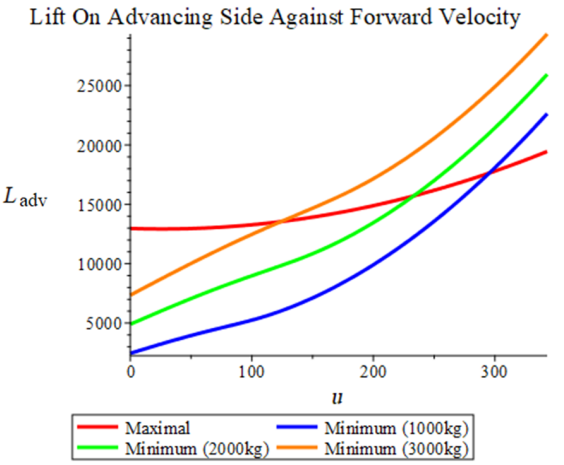

FIGURE 13. Plot of the average lift over the advancing half of the helicopter rotor disk against forward velocity.

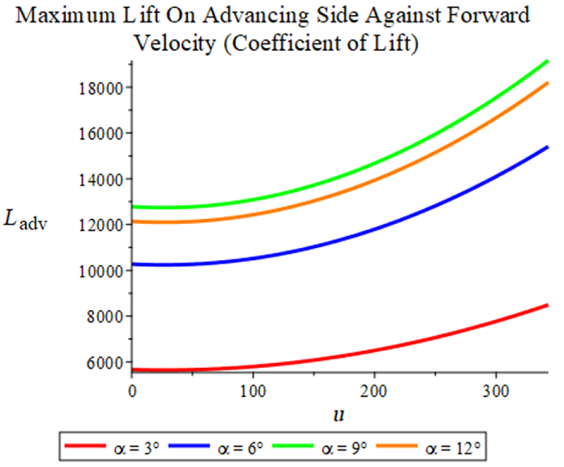

FIGURE 14. Plot of the average lift over the advancing half of the helicopter rotor disk against forward velocity for several angles of attack.

To elucidate the effect of the angle of attack on the advancing side of the blade, we multiply the lift by the coefficient of lift using the maximal values for Ω. In Figure 14, we see lower angles of attack predictably produce less lift up to the stall threshold $\alpha_c \approx 10°$. When the angle of attack exceeds this limit, the lift begins to decrease, as expected with retreating blade stall.

To additionally incorporate the effect of drag, we alter the integral on the advancing blades with the proportion $(C_L(\alpha) - C_D(\alpha))$. Given that drag increases sharply with

https://doi.org/10.1017/S1446181123000081 Published online by Cambridge University Press

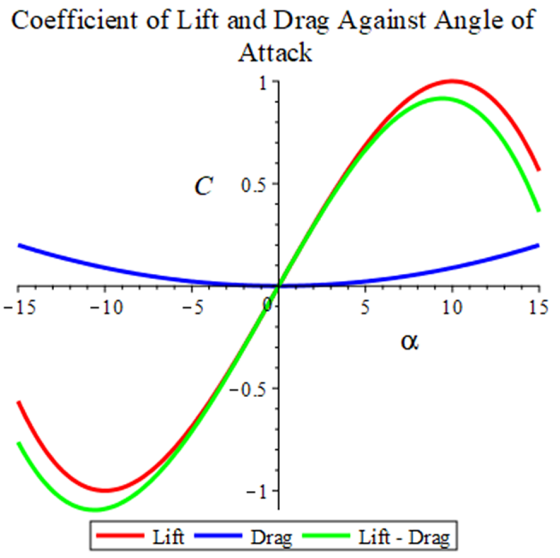

FIGURE 15. Plot of the lift coefficient and the difference between lift and drag against the angle of attack.

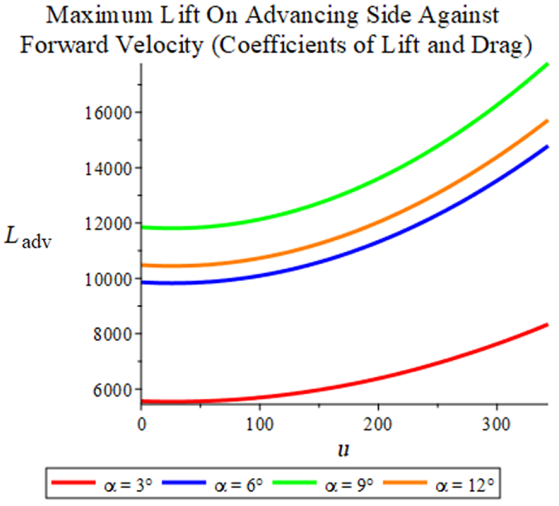

FIGURE 16. Plot of the average lift over the advancing half of the helicopter rotor disk against forward velocity for several angles of attack.

the angle of attack, we expect an optimal angle of attack that allows the greatest lift coefficient under the drag coefficient, as shown in Figure 15.

Figure 16 shows the lift on the advancing side with the coefficient of drag included in the computation. Though the effect of the drag is slight, the increased angle of attack magnifies the gap between the lift at $\alpha = 9°$ and $\alpha = 12°$.

https://doi.org/10.1017/S1446181123000081 Published online by Cambridge University Press

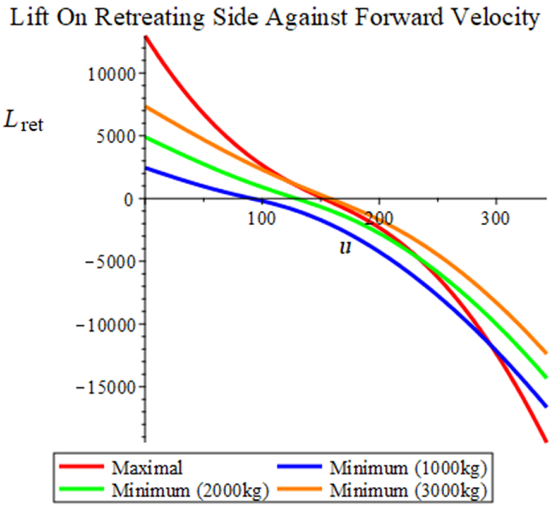

FIGURE 17. Plot of the average lift over the retreating half of the helicopter rotor disk against forward velocity.

3.7. Lift on the retreating side of the rotor disk To obtain the lift generated on the retreating side of the rotor disk, we calculate

$$L_{\text{ret}}(u) = \frac{1}{\pi}\int_{\pi/2}^{3\pi/2}\int_{0}^{R}\frac{1}{2}\rho c(\Omega r + u\cos(\theta))|\Omega r + u\cos(\theta)|\,dr\,d\theta.$$

Given that $\Omega r + u\cos(\theta)$ is not necessarily nonnegative nor nonpositive, there is no simplification. To calculate this integral, we use MAPLE's built-in numerical integration with a partition of 100 points. In Figure 17, the retreating lift can be seen to rapidly decrease. Without measures to nullify negative lift, the retreating side continues to build negative lift as forward velocity increases. For coaxial helicopters, Figure 13 shows us that the lift increase from the advancing side is more than capable of balancing the lift loss on the retreating side.

3.8. Angle of attack considerations for coaxial helicopters In our previous mathematical derivations for the lift across the rotor disk (or particular regions of the rotor disk), we have assumed that the coefficient of lift constantly takes its maximum value $C_L = 1$. In this section, we relax this assumption to derive conditions on the coefficient of lift that will enable the lift to be generated equally across the rotor disk.

For low forward velocities, we are able to apply the simple formula

$$C_L(\theta) = \frac{L}{L_{\text{std}}(u,\theta)},$$

https://doi.org/10.1017/S1446181123000081 Published online by Cambridge University Press

where $L_{\text{std}}(u,\theta)$ is the lift generated by the blade at forward velocity u and azimuth angle θ, given by

$$L_{\text{std}}(u,\theta) = \frac{\rho c}{6\Omega}[(\Omega R + u\cos(\theta))^2|\Omega R + u\cos(\theta)| - u^3\cos^2(\theta)|\cos(\theta)|].$$

This expression remains valid until the lift generated on the retreating blade is no longer capable of producing sufficient lift. That is, the first threshold is the forward velocity u_1 such that

$$L_{\text{std}}(u_1,\pi) = L.$$

Assuming the rotor angular velocity is at its maximum, as shown by equation (1.1), we may simplify the above equation to show u_1 satisfies

$$u_1^3 - \frac{4}{3}\nu u_1^2 - \frac{2}{3}\left(\nu^2 + \frac{L}{\rho c R}\right)u_1 - \frac{\nu}{9}\left(\nu^2 - \frac{6L}{\rho c R}\right) = 0.$$

For velocities $u > u_1$, we set the angle of attack on the retreating blades to maximum and increase the angle of attack on the counterpart advancing blade to compensate for the insufficient lift generation.

3.8.1. Lift compensation for retreating blades As the forward velocity u increases above the first threshold u_1 defined above, we must produce excess lift on the advancing blades to compensate for the lack of lift produced on the retreating blades. Suppose each blade must generate L lift. If $u < u_1$, $L_{\text{std}}(u,\pi) < L$. Therefore, the excess lift E that the advancing blades must produce is given by

$$E = L - L_{\text{std}}(u,\pi).$$

In Figure 18, we see the lift compensation E that the advancing blade must produce for its counterpart retreating blade. The curves in Figure 18 are proportional to the maximum lift produced in hover that the highest weight helicopters may attain. Negative values indicate the retreating blade is producing sufficient lift, and compensation is not necessary. As the forward velocity increases, the critical values $E(u) = 0$ coincident with $u_1(L)$ are found. The lift compensation required also increases up to the critical value $\nu/3$.

Therefore, in the case that $u > u_1(L)$, the coefficient of lift will take the form

$$C_L(\theta) = \begin{cases} \dfrac{2L - \min\left(\dfrac{L}{L_{\text{std}}(u,\theta+\pi)}, 1\right)L_{\text{std}}(u,\theta+\pi)}{L_{\text{std}}(u,\theta)}, & \theta \in \left[0,\dfrac{\pi}{2}\right] \cup \left[\dfrac{3\pi}{2}, 2\pi\right], \\ \min\left(\dfrac{L}{L_{\text{std}}(u,\theta)}, 1\right), & \theta \in \left[\dfrac{\pi}{2}, \dfrac{3\pi}{2}\right]. \end{cases}$$

3.8.2. Speed limit imposed on transitioning blades Consider the lift produced by the blades as they transition between the advancing and retreating halves of the rotor

https://doi.org/10.1017/S1446181123000081 Published online by Cambridge University Press

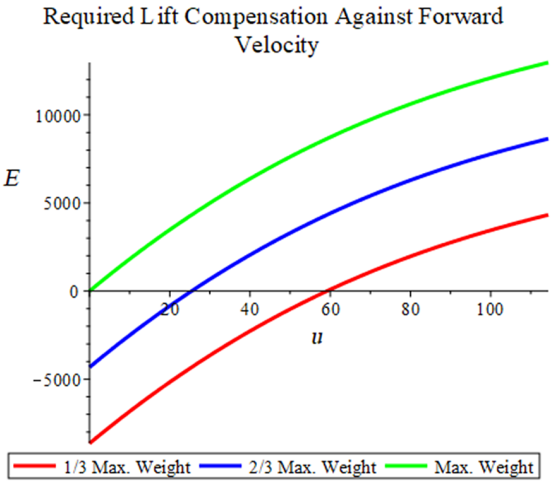

FIGURE 18. Plot of the average lift over the retreating half of the helicopter rotor disk against forward velocity.

disk (at azimuth angles 90° and 270°). The lift produced on these blades is equal and unaffected by the forward velocity. That is,

$$L_{\text{std}}\left(u, \frac{\pi}{2}\right) = L_{\text{std}}\left(u, \frac{3\pi}{2}\right) = \frac{\rho c R^3 \Omega^2}{6}.$$

Since the rotor angular velocity Ω decreases as forward velocity u increases, the lift produced on the transitioning blades decreases. For a given lift L, with the maximal rotor angular velocity Ω given in equation (1.1),

$$\frac{\rho c R}{6}(v - u)^2 = L.$$

Solving for u,

$$u = v - \sqrt{\frac{6L}{\rho c R}}. \tag{3.4}$$

We plot the maximum speed limit as a function of lift in Figure 19. As we increase the amount of lift the blade must produce, the maximum forward velocity at which the blades are able to maintain the lift decreases. Therefore, coaxial helicopters are subject to an additional speed limit in equation (3.4) as imposed by the reduced lift on the transitioning blades. Though using four blades per disk reduces the lift demand for each blade, the problem of reduced lift on transitioning blades remains, as seen in Figure 20.

https://doi.org/10.1017/S1446181123000081 Published online by Cambridge University Press

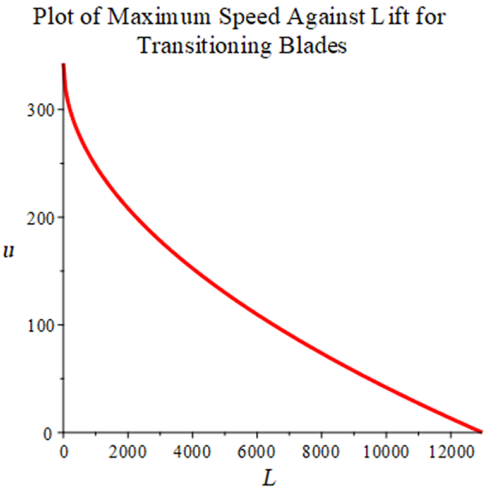

FIGURE 19. Plot of the maximum speed limit imposed by equation (3.4) against lift.

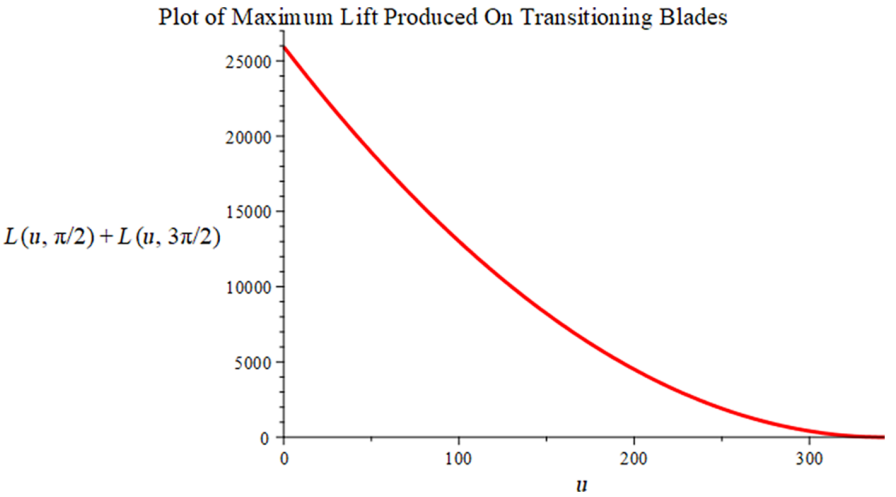

FIGURE 20. Plot of the maximum lift produced by the blades at $\theta = 90°$ and $\theta = 270°$.

4. Conclusion

From the various models for the lift equation, we conclude that replacing the v^2 term with $v|v|$ is recommended to capture the effect of the stall region about the rotor shaft on the retreating side (as seen in Figures 5 and 6). The lift dynamics at higher forward velocities are also better modelled by the modified velocity term. In the ideal lift situation, we find that the retreating blade produces no lift for the forward velocity $u = v/3$, regardless of R. This implies conventional helicopters with one main

https://doi.org/10.1017/S1446181123000081 Published online by Cambridge University Press

rotor cannot accelerate to $v/3 \approx 114.3\,\mathrm{ms}^{-1}$, and struggle to handle dissymmetry of lift at speeds close to $v/3$. We use equation (3.2) to find the minimum rotor angular velocity required to generate L lift. To avoid supersonic blade issues, the rotor speed Ω must decrease when the forward velocity u increases. Because of this, the overall lift is decreased, as shown in Figure 10. For the proposed coaxial design featuring two counter-rotating blades, no lift will be produced on the retreating blades. This impacts the lift generated by the helicopter, as shown in Figure 10.

Acknowledgements

The authors would like to acknowledge Hyper Q Aerospace for their support. They would also like to thank Graeme Hocking for his input and for his moderation of the related project at MISG 2020.

References

[1] J. Fay, *The helicopter*, 4th edn (Hippocrene Books, New York, 1987).
[2] W. Johnson, *Helicopter theory* (Dover Publications, Inc., New York, 1994); https://books.google.com.au/books?id=SgZheyNeXJIC&pg=PA7&source=gbs_selected_pages&cad=2#v=onepage&q&f=false.
[3] A. Kulchenko, V. Kostukov, L. Verevkina and V. Chufistov, "The features of flight dynamic single rotor helicopter mathematical model: for application in autopilots that based on position-trajectory algorithms", *2014 19th Int. Conf. on Methods and Models in Automation and Robotics (MMAR)* (IEEE, Miedzyzdroje, Poland, 2014) 423–428; doi:10.1109/MMAR.2014.6957391.
[4] M. La Mantia and P. Dabnichki, "Effect of the wing shape on the thrust of flapping wing", *Appl. Math. Model.* **35** (2011) 4979–4990; doi:10.1016/j.apm.2011.04.003.
[5] G. J. Leishman, *Principles of helicopter aerodynamics with CD extra* (Cambridge University Press, Cambridge, 2006).
[6] X. Liu, S. Liang, G. Li, A. Godbole and C. Lu, "An improved dynamic stall model and its effect on wind turbine fatigue load prediction", *Renew. Energy* **156** (2020) 117–130; doi:10.1016/j.renene.2020.04.040.
[7] J. R. Majhi and R. Ganguli, "Helicopter blade flapping with and without small angle assumption in the presence of dynamic stall", *Appl. Math. Model.* **34** (2010) 3726–3740; doi:10.1016/j.apm.2010.02.010.
[8] NACA0012 airfoils, (n0012-il). http://airfoiltools.com/airfoil/details?airfoil=n0012-il#polars.
[9] O. Perdomo and F. Wei, "On the flapping motion of a helicopter blade", *Appl. Math. Model.* **46** (2017) 299–311; doi:10.1016/j.apm.2017.01.055.
[10] G. Romani and D. Casalino, "Rotorcraft blade-vortex interaction noise prediction using the lattice-Boltzmann method", *Aerosp. Sci. Technol.* **88** (2019) 147–157; doi:10.1016/j.ast.2019.03.029.
[11] K. V. Rozhdestvinsky and V. A. Ryzhov, "Aerohydrodynamics of flapping-wing propulsors", *Prog. Aerosp. Sci.* **39** (2003) 585–633; doi:10.1016/S0376-0421(03)00077-0.